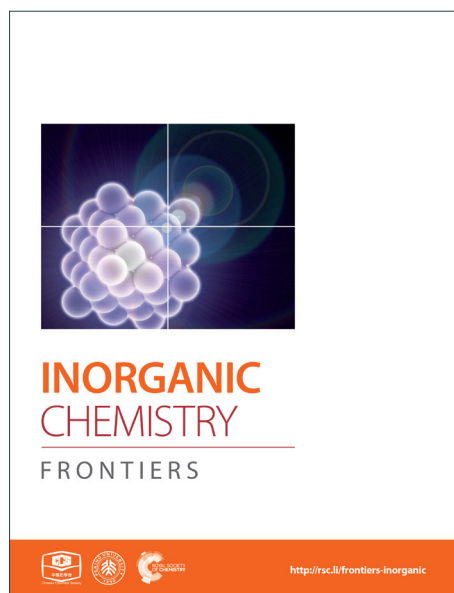
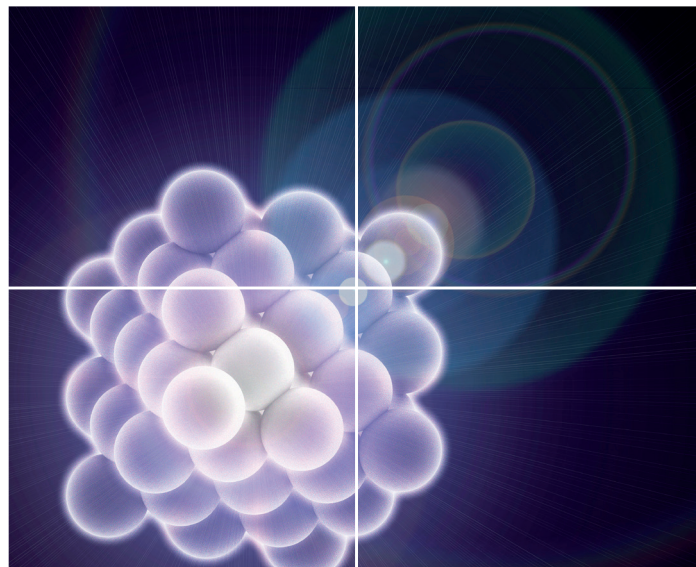


INORGANIC CHEMISTRY

FRONTIERS

Accepted Manuscript



This is an *Accepted Manuscript*, which has been through the Royal Society of Chemistry peer review process and has been accepted for publication.

Accepted Manuscripts are published online shortly after acceptance, before technical editing, formatting and proof reading. Using this free service, authors can make their results available to the community, in citable form, before we publish the edited article. We will replace this *Accepted Manuscript* with the edited and formatted *Advance Article* as soon as it is available.

You can find more information about *Accepted Manuscripts* in the [Information for Authors](#).

Please note that technical editing may introduce minor changes to the text and/or graphics, which may alter content. The journal's standard [Terms & Conditions](#) and the [Ethical guidelines](#) still apply. In no event shall the Royal Society of Chemistry be held responsible for any errors or omissions in this *Accepted Manuscript* or any consequences arising from the use of any information it contains.

ARTICLE

Highly Fluorescent Zinc Complex of Dipodal N-Acyl hydrazone as a Selective Sensor for H_2PO_4^- ion and Application in Living Cells

Cite this: DOI: 10.1039/x0xx00000x

Received 00th January 2012,

Accepted 00th January 2012

DOI: 10.1039/x0xx00000x

www.rsc.org/Sivalingam Suganya^a, Sivan Velmathi^{a*}, Parthiban Venkatesan^b, Shu-Pao Wu^b and Maria Susai Boobalan^c

A dipodal N-acyl hydrazone receptor (**R1**) was synthesized in a single step, and utilized as test probe for the selective sensing of metal ion as well as anion. Upon the exposure of various metal ions, **R1** display a rapid colorimetric and absorption changes in presence of Co^{2+} , Ni^{2+} , Cu^{2+} and Zn^{2+} ions. However, **R1** show selective fluorescent response only in presence of Zn^{2+} ion and no other metal ions showed obvious changes. In particular, zinc acetate showed higher sensitivity over other zinc sources. Upon the binding of Zn^{2+} ion with **R1**, colorless solution was changed into fluorescent yellow color accompanied with non-fluorescent nature into highly fluorescent nature. The insitu formed **R1**- Zn^{2+} complex was further explored for the reversible recognition of H_2PO_4^- ion selectively over other anions such as F^- , Cl^- , Br^- , AcO^- , CN^- , HSO_4^- and NO_3^- ions. A strong and enhanced emission at 502 nm and 534 nm corresponds to **R1**- Zn^{2+} complex was quenched completely in presence of H_2PO_4^- ion. Relay recognition of different phosphates such as mono, di and tri basic phosphate ions also tested. Furthermore, **R1** have good cell permeability and could serve as a bio probe in living cells for the intracellular uptake of Zn^{2+} and H_2PO_4^- ions. Time dependent density functional (TDDFT) calculation has been performed to demonstrate the binding of Zn^{2+} ion with **R1**.

Introduction

To develop the test probe for the biologically important metal ion and anions have gained increasing attention due to their imperative role in biological and environmental applications¹⁻³. Among transition metal ions, cobalt⁴⁻⁵, nickel⁶⁻⁷, copper⁸⁻¹³ and zinc¹⁴⁻¹⁵ are the essential elements to the human body due to their highly important role in bio processes such as neural transmission, gene transcription, electron transfer and metabolic process. Also, Cu^{2+} and Zn^{2+} ion are found as the main catalytic component of many enzyme hydrolyzed and redox reactions which are also helpful for the protein synthesis and DNA synthesis. At the same time, decreased concentration of these metal ions may cause disease like Alzhiemer, osteoporosis, Wilson's disease, Parkinson's disease, chronic liver and renal disease, diabetes, malignancy and infantile diarrhoea. They are also required for the normal growth of cells during pregnancy, childhood and adolescence.

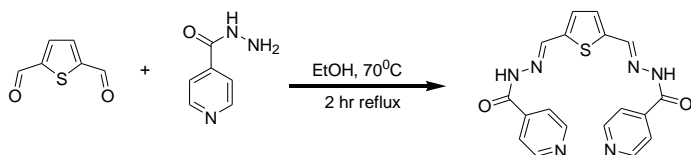
Previously, analytical methods like, ICP-MS, AAS and EPR are available for the quantification of metal ions, however they are undesirable in terms of their higher cost, precise results, more analysis time and need different sources for each metal ions.

Particularly, identification of diamagnetic metal ions is not an easy process using these analytical techniques. Colorimetric analysis and fluorescence spectroscopic technique¹⁶⁻²¹ can avoid this problem in the testing of diamagnetic Zn^{2+} ion with high sensitivity. The analyte recognition using fluorescence spectroscopy is mainly following "turn-on" or "turn-off" mechanism. Still, to design a "turn-on" fluorescence sensor is highly challenging, thus giving a bright signal in the dark background. Equally, recognition of bio active anions also came into limelight since they play significant roles in bio process. In particular, phosphates are the crucial anions since it is used as energy storage device and signal transducers. Apart, phosphates are the well known anions used in the industrial process. Hence the phosphates ion detection has gained great demand²²⁻²⁵. Currently relay recognition²⁶ approach has been implemented for the selective sensing of anions using insitu formed metal complex. Although different metal complexes²⁷⁻³⁴ are reported for the detection of phosphate ion, reports on Zn^{2+} ensemble for the selective sensing of phosphate ion is still limited³⁵⁻³⁸. Utilizing the strong affinity of phosphate ion towards Zn^{2+} ion, recently Shi et al.³⁹ has reported Zn^{2+} ensemble for the detection of H_2PO_4^- ion. Datta et al.⁴⁰ and Liang et al. have reported Zn^{2+} complex for the selective sensing of pyrophosphate (PPI) ion⁴¹.

Small molecules synthesis is always welcome, because they can be synthesized in a single step which avoids the problems like high cost, disposal of hazardous chemicals and solvents. With the extension of our research in chemosensors field using dipodal receptor⁴²⁻⁴⁵, we have synthesized a new dipodal N-acyl hydrazone (**R1**) in a single step and applied for the forward recognition of Zn^{2+} ion and backward recognition of H_2PO_4^- ion. **R1** shows clear colorimetric and UV-vis changes towards Co^{2+} , Ni^{2+} , Cu^{2+} and Zn^{2+} ions. However, **R1** display remarkable fluorescence enhancement only in presence of Zn^{2+} ion over other metal ions. Further the **R1**- Zn^{2+} complex was used as test probe for the reversible recognition of H_2PO_4^- ion of Tetra butyl ammonium (TBA) salt selectively. Similarly, potassium salts of phosphates with different basicity also recognized using **R1**- Zn^{2+} complex. With the aid of fluorescence spectroscopy, **R1** was successfully tested as a bio probe towards the intracellular uptake of Zn^{2+} and H_2PO_4^- ion in the living RAW264.7 cells. Theoretically calculated energy values was compared with the absorbance corresponds to **R1** and **R1**- Zn^{2+} complex obtained from UV-vis spectrum.

Results and Discussion

R1 was synthesized in a single step and well characterized using spectroscopic techniques. The evaluation on binding ability of **R1** toward metal ions and phosphate ion has been performed using colorimetric, UV-vis and fluorescence experiments. Utilizing the fluorescence response, testing of H_2PO_4^- ion in living cells was performed using **R1**- Zn^{2+} complex.



Scheme-1 Synthesis of **R1**

Metal ion recognition: Colorimetric, UV-vis and fluorescence spectroscopy

Colorimetric recognition of any analyte is still a challenging and interesting task due to their quick response in visual changes upon binding with organic receptor. Acetate salts of Mn^{2+} , Co^{2+} , Ni^{2+} , Cu^{2+} , Zn^{2+} , Pb^{2+} , Na^+ and TBA⁺ (1.5 mM in H_2O) were taken for the analysis. When 2 eq. of different metal acetate and TBAAc were added to the DMSO solution of **R1** (50 μM), rapid color changes were observed from colorless to yellow for Co^{2+} , Ni^{2+} , Cu^{2+} and Zn^{2+} ions. Acetate salts of other counter cations were not showed significant colorimetric changes (Fig. 1). Such spontaneous color changes clearly suggest, **R1** could serve as colorimetric probe for these metal ions. Such visible color change is mainly because of the formation of coordination complexes with **R1**.



Fig. 1 Colorimetric changes of **R1** (50 μM in DMSO) upon the addition of 2 eq. of various acetate salts of cations (1.5 mM in H_2O).

To further insight into the metal ion coordination with **R1**, UV-vis titration was employed. **R1** displays a strong absorption at 383 nm due to intramolecular charge transfer (ICT)⁴⁶⁻⁴⁸ within the molecule. As shown in Fig. 2, upon the addition of different metal salts, a strong absorption band was observed in the visible region at 431 nm, 447 nm, 450 nm and 450 nm in presence of Co^{2+} , Ni^{2+} , Cu^{2+} and Zn^{2+} respectively. Meanwhile the absorption intensity at 383 nm decreased with the increasing concentration of metal ions. Further the uniform formation of coordination complex with **R1** was investigated with the incremental addition (0-2 eq.) of these specific metal ions and absorption spectrum was recorded (Fig. 3). In solution phase, N-acyl hydrazone undergo isomerisation⁴⁹⁻⁵⁰. The isomerization takes place through acylhydrazone-azo tautomerization which leads to the formation of OH functional group. During the complexation process, the metal ions deprotonate the OH group present in isomerized **R1** and coordinate with the oxygen anion as well as imine nitrogen. The red shift in the absorption band at 383 nm to around 450 nm confirms the coordination of metal ions with **R1**. The single isobestic point observed in the absorption spectra clearly revealing the presence of two species such as free **R1** and metal ions bound **R1**.

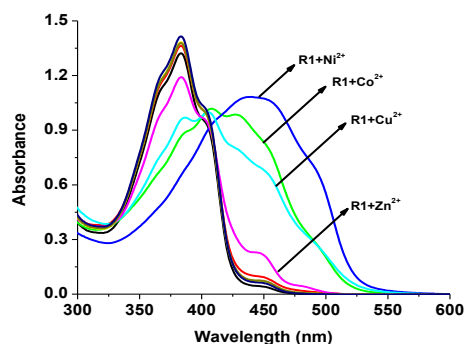


Fig. 2 UV-vis changes of **R1** (50 μM in DMSO) upon the addition of 2 eq. of various acetate salts of cations (1.5 mM in H_2O).

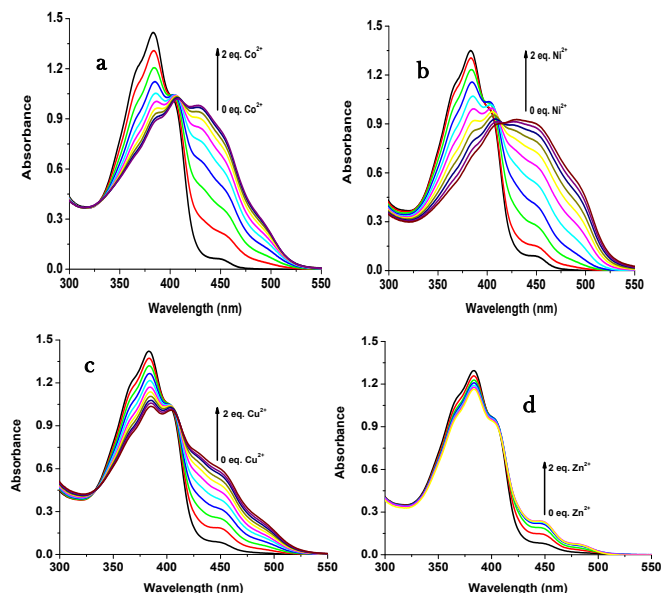


Fig. 3 UV-vis changes of **R1** (50 μM in DMSO) upon the addition of 0-2 eq. of (a) Co^{2+} , (b) Ni^{2+} , (c) Cu^{2+} and (d) Zn^{2+} ions (1.5 mM in H_2O).

In order to study the sensitivity of **R1** towards selective metal ion, fluorescence titration was carried out. Free **R1** did not show significant fluorescent signal with the excitation at 440 nm. The non-fluorescent nature of **R1** is mainly due to the presence of ICT and the free rotation of **R1** around azomethine ($\text{CH}=\text{N}$) bond. When **R1** was exposed towards different metal acetate such as $\text{Mn}(\text{OAc})_2$, $\text{Co}(\text{OAc})_2$, $\text{Ni}(\text{OAc})_2$, $\text{Cu}(\text{OAc})_2$, $\text{Pb}(\text{OAc})_2$, $\text{Na}(\text{OAc})$ and TBAAC, no significant response was found in emission spectrum. Even though Co^{2+} , Ni^{2+} and Cu^{2+} showed colorimetric and absorption changes, they were also not showing any significant emission changes which clearly suggesting the formation of only ground state complex. Surprisingly only the presence of Zn^{2+} ion showed remarkable fluorescence enhancement with two maxima at 502 nm and 534 nm (Fig. 4). The enhanced fluorescence intensity upon the complexation of **R1** with Zn^{2+} is mainly due to the intramolecular charge transfer (ICT) and chelation enhanced fluorescence (CHEF) effect⁵⁰. The chelation of Zn^{2+} ion with the isomerized **R1** resulting in more rigidity of the molecule via inhibiting the free rotation of **R1** around $\text{CH}=\text{N}$ bond and arresting the lone pair of electrons present in imine nitrogen. Consequently, both imine nitrogen and the electron donating nature of deprotonated oxygen anion would be greatly increased which makes the possible coordination of Zn^{2+} ion. Due to the rigid conjugation caused by the CHEF effect, emission is taking place within the thiophene fluorophore and gives the enhanced fluorescence intensity at 502 nm and 534 nm. Zn^{2+} ion was found to form both ground as well as excited state complex with **R1**, thus giving a remarkable fluorescence enhancement. With the increasing concentration of 0-2 eq. of Zn^{2+} ion, gradual increase in the emission bands at 502 and 534 nm was observed (Fig. 5). FTIR spectrum also clearly supports the complexation of Zn^{2+} ion with **R1**. Free **R1** exhibits the band at 3213 cm^{-1} , 1646 cm^{-1} and 1544 cm^{-1} corresponds to NH , $\text{C}=\text{O}$, and $\text{CH}=\text{N}$ functional groups. Upon the complexation with Zn^{2+} ion, the band at 3213 cm^{-1} disappeared and the bands at 1646 cm^{-1} and 1544 cm^{-1} was shifted into 1590 cm^{-1} and 1519 cm^{-1} respectively. This results clearly suggests that the $\text{O}=\text{C}-\text{NH}$ undergone isomerisation into $\text{HO}-\text{C}=\text{N}$ and thus the incoming Zn^{2+} ion form a stable complex with deprotonated oxygen anion and imine nitrogen atom.

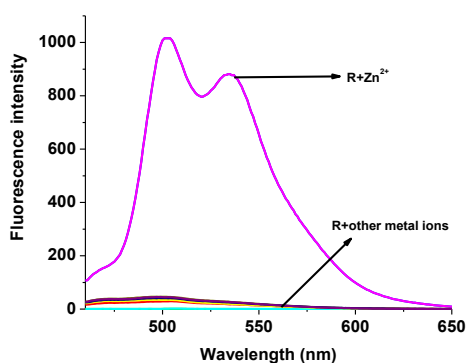


Fig. 4 Fluorescence changes of **R1** (50 μM in DMSO) upon the addition of (a) 2 eq. of various acetate salts of cations (1.5 mM in H_2O).

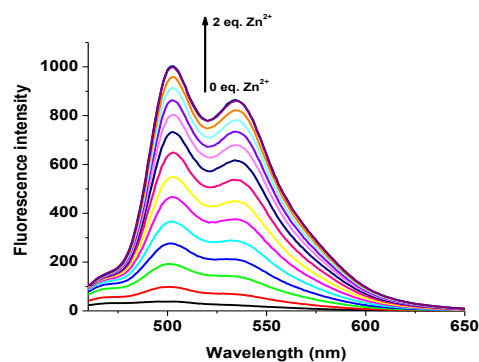


Fig. 5 Fluorescence changes of **R1** (50 μM in DMSO) upon the addition of 0- 2 eq. of $\text{Zn}(\text{OAc})_2$ (1.5 mM in H_2O).

Specific sensing of $\text{Zn}(\text{OAc})_2$

To get a deep insight into the selective and specific sensing of $\text{Zn}(\text{OAc})_2$, fluorescence titration was carried out using other zinc salts also. As shown in Fig. 6, addition of 2 eq. of aqueous solution of $\text{Zn}(\text{OAc})_2$ to the solution of **R1**, strong emission at 502 nm and 534 nm with maximum intensity was produced. Whereas, addition of other zinc salts such as ZnCl_2 , $\text{Zn}(\text{NO}_3)_2$ and ZnBr_2 displayed 5-20 fold less fluorescence intensity than that of $\text{Zn}(\text{OAc})_2$. The quantum yield was measured with rhodamine B as a reference ($\Phi=0.69$). Quantum yield was found to be $\Phi=0.01$ for **R1** alone, and for the complexes of **R1**- $\text{Zn}(\text{OAc})_2$, ZnCl_2 , ZnBr_2 and $\text{Zn}(\text{NO}_3)_2$ were 0.726, 0.124, 0.083 and 0.036 respectively. These results strongly suggest that the higher basicity of $\text{Zn}(\text{OAc})_2$ make feasible coordination with **R1** over other zinc sources.

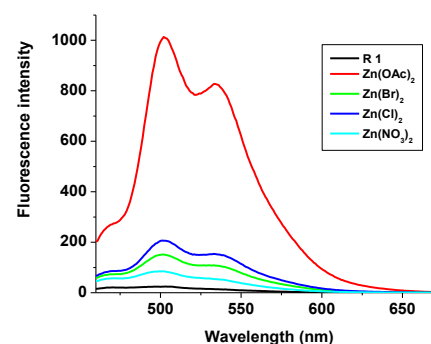


Fig. 6 Fluorescence changes of **R1** (50 μM in DMSO) upon the addition of 2 eq. $\text{Zn}(\text{OAc})_2$, ZnCl_2 , $\text{Zn}(\text{NO}_3)_2$ and ZnSO_4 (1.5 mM in H_2O).

Reversible recognition of H_2PO_4^- ion

Fluorescent **R1**- Zn^{2+} complex was further explored as secondary sensor system towards anions recognition via relay recognition approach. With the knowledge of strong interactions between Zn^{2+} and H_2PO_4^- ion, **R1**- Zn^{2+} ensemble was expected to act as an efficient system for H_2PO_4^- ion detection. To evaluate the selective detection of H_2PO_4^- ion, various anions such as F^- , Cl^- , Br^- , CN^- , AcO^- , HSO_4^- and NO_3^- were added to the solution of **R1**- Zn^{2+} complex. Interestingly, the yellow color of **R1**- Zn^{2+} complex was

turned into colorless only with the addition of H_2PO_4^- ion (Fig. 7). Simultaneously, the presence of H_2PO_4^- ion makes rapid quenching in the fluorescence intensity at 502 nm and 534 nm resulting in free R1 (Fig. 8). Other anions did not show any obvious changes in the colorimetric or fluorescence response. Addition of 0-2 eq. of H_2PO_4^- ion show gradual quenching in the fluorescent intensity at 502 and 534 nm led to non-fluorescent in nature which indicates the revival of ICT process (Fig. 9). This is the stronger complexation because of the strong interaction of H_2PO_4^- ion with Zn^{2+} than the complexation of Zn^{2+} with deprotonated N anion. These results strongly suggesting the sequestration of Zn^{2+} ion from the ensemble and regenerate free R1 and form $\text{Zn}(\text{H}_2\text{PO}_4)_2$ complex. Simultaneously, relay recognition of phosphates with different basicity also performed using KH_2PO_4 , K_2HPO_4 and K_3PO_4 (Fig. 10). Presence of all the three phosphates quenches the fluorescence intensity of R1- Zn^{2+} complex. However, the order of fluorescence quenching depending on the basicity was found to be $\text{KH}_2\text{PO}_4 > \text{K}_2\text{HPO}_4 > \text{K}_3\text{PO}_4$. Addition of 2 eq. of KH_2PO_4 shows similar results like TBAH_2PO_4 salt.



Fig. 7 Colorimetric changes of R1- Zn^{2+} complex (50 μM in DMSO) upon the addition of 2 eq. of various anions (1.5 mM in H_2O).

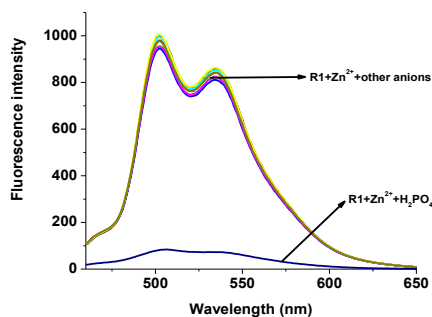


Fig. 8 Fluorescence changes of R1- Zn^{2+} complex (50 μM in DMSO) upon the addition of 2 eq. of various anions (1.5 mM in H_2O).

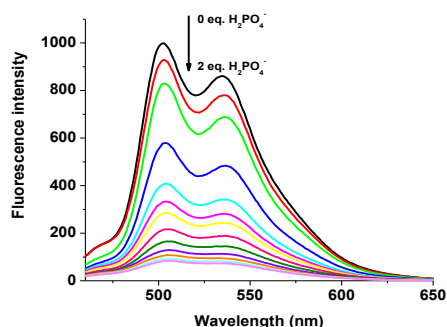


Fig. 9 Fluorescence changes of R1- Zn^{2+} complex (50 μM in DMSO) upon the addition of 0-2 eq. of H_2PO_4^- (1.5 mM in H_2O).

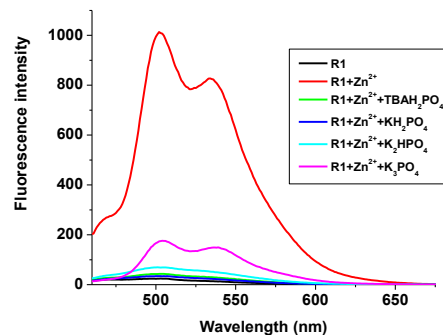


Fig.10 Fluorescence changes of R1- Zn^{2+} complex (50 μM in DMSO) upon the addition of 0-2 eq. of different phosphate sources (1.5 mM in H_2O).

Fluorescence detection of Zn^{2+} and H_2PO_4^- ions in Living Cells

The fluorescence detection of Zn^{2+} and H_2PO_4^- ions in cell line RAW264.7 were performed by bio imaging process in TBS and Dulbecco's modified Eagle's medium (DMEM). Culture media (2 ml) was added to the cell culture, which was treated with the solution of R1 (10 μM in DMSO) and the samples were incubated at 37 $^\circ\text{C}$ for 30 min, and then washed with TBS buffer before imaging. R1 supplemented living cells alone did not induce any fluorescence imaging. The uptake of Zn^{2+} (10 μM) ion by R1 supplemented cells was performed in TBS buffer (pH 7.4) and incubated for 30 min at 37 $^\circ\text{C}$, the excess metal ions was removed by TBS buffer. The interaction of Zn^{2+} ion with R1, generated green fluorescence in the cells was imaged by confocal microscope. Further, the successive interaction of H_2PO_4^- ion (20 μM) towards R1- Zn^{2+} complex was performed. The green fluorescence was turned off upon the introduction of H_2PO_4^- ion (Fig. 11). The obtained bio imaging results are in well agreement with the fluorescence spectra towards both Zn^{2+} and H_2PO_4^- ions recognition. This bio analysis reveals the good cell permeability of R1, which can be further explored as a biomaterial for the probing of bioactive analytes in the cellular environment. With the results of fluorescence titrations and bioimaging analysis, the binding mechanism was proposed as

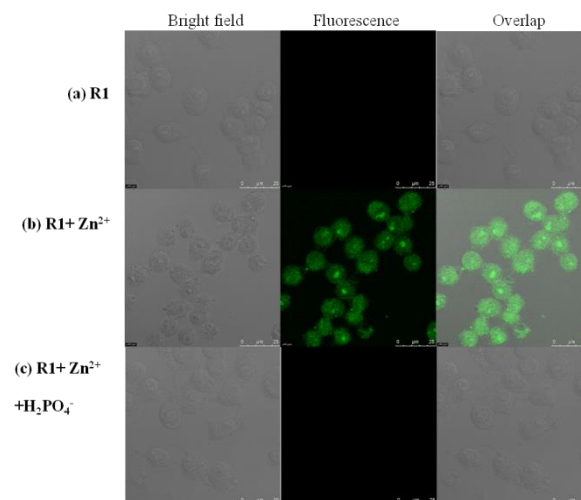


Fig.12.

Fig.11. Fluorescence images of macrophage (RAW 264.7) cells treated with **R1**, Zn^{2+} and H_2PO_4^- . (Left) Bright field image; (Middle) fluorescence image; and (Right) merged image. (Ex 447nm, Em.502-534nm.)

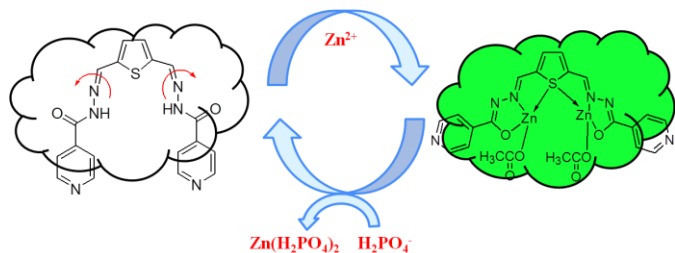


Fig. 12 Proposed mechanism for the reversible sensing of H_2PO_4^- ions by **R1**- Zn^{2+} complex.

2:1 (metal ion: **R1**) binding mode was confirmed by Job's plot. Table 1 describes the association constant (K_a) values calculated using Benesi-Hildebrand (B-H) method and detection limit values calculated using the formula $3^*\sigma/m$. Where, σ is the standard deviation of 10 blank samples and 'm' is the slope.

Metal ions	K_a	LOD	Stoichiometry
Co^{2+}	6.74×10^4	^a 4.24 μM	2:1
Ni^{2+}	1.20×10^4	^a 5.12 μM	2:1
Cu^{2+}	4.44×10^4	^a 8.47 μM	2:1
Zn^{2+}	2.06×10^5	^a 1.86 μM , ^b 3.79 nM	2:1
H_2PO_4^-		^b 1.80 nM	

a-absorption measurement, b-emission measurement.

Table. 1 Association constants (K_a), detection limit and stoichiometry of **R1** with Co^{2+} , Ni^{2+} , Cu^{2+} and Zn^{2+} ions.

TDDFT calculation

To get in-depth knowledge in the electronic transition of **R1** and **R1**- Zn^{2+} complex, density functional theory (DFT) combined with time-dependent density functional theory (TDDFT)⁵¹ calculations were done using Gaussian09 program package⁵² and the energies were compared with experimental observation. Time Dependent Density Functional Theory is one of the most important quantum chemical treatments to investigate structure, properties and dynamics of excited systems. DFT based Beck-3 Lee Young Parr (B3LYP)/6-31G(d,p) model chemistry and effective core potential (ECP) based LANL2DZ basis set was incorporated for the **R1** and **R1**- Zn^{2+} complex. **R1** act as tridentate donor via N, O, S coordination

site and thus it can easily coordinate with Zn^{2+} ion. The energies between HOMO (highest occupied molecular orbital) and LUMO (lowest unoccupied molecular orbital) of **R1** and **R1**- Zn^{2+} complex were calculated from the optimized structure of the same (Fig.13 and S6). UV-vis spectra display, absorption band of **R1** was red shifted when it undergo complexation with Zn^{2+} ion. TDDFT calculation also clearly supports the above experimental results, the energy gap between HOMO to LUMO was reduced for **R1**- Zn^{2+} (2.18eV) complex than that of free **R1** (2.761 eV). Further to explain the electronic transition, the reduced energy gap of HOMO-LUMO was correlated with the emission observed. In **R1**, TDDFT calculation predicts the first singlet transition S_0 - S_1 with 2.761 eV. S_0 and S_1 levels are dominated by HOMO to LUMO, where HOMO level is contributed to the electron localised imine moiety and LUMO level is contributed to the thiophene fluorophore. The imine nitrogen contains lone pair of electrons is closely connected at the two arms of thiophene fluorophore. Upon the excitation of free **R1**, there is a possibility of electron transfer from HOMO level of imine nitrogen to HOMO level of fluorophore, thus weak emission was caused. When **R1** binds with Zn^{2+} ion, the transfer of lone pair of electrons are inhibited, consequently the HOMO level of imine decreased than the HOMO level of fluorophore. Thus, the electronic transition in case of **R1**- Zn^{2+} complex takes place within the fluorophore (S_1 - S_0) which gives strong emission (Fig. 14).

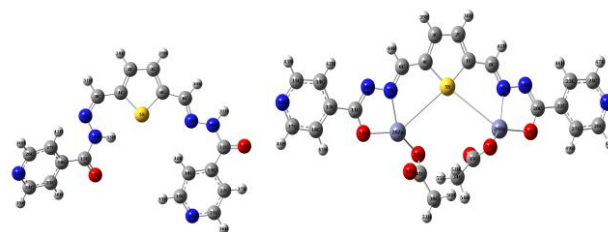


Fig. 13. Optimized geometries of **R1** and **R1**- Zn^{2+} complex.

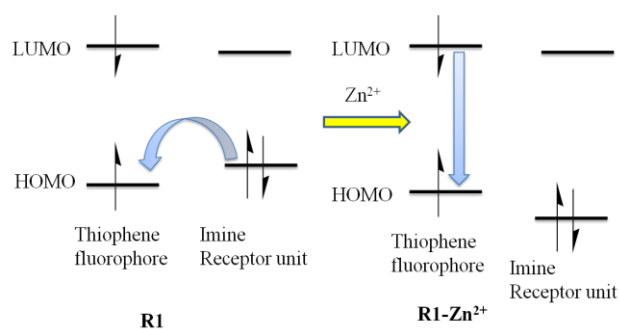


Fig. 14 Electronic transitions in **R1** and **R1**- Zn^{2+} complex.

Experimental Section

Materials and Instruments

All the starting materials and solvents used for the synthesis and titration purpose were received commercially and used as such. All the metal acetate salts, different potassium phosphate

salts and tetra butyl ammonium salts of anions were received as commercial materials and used without any further purification. ^1H and ^{13}C NMR spectra were obtained on a BRUKER AV III-400 MHz Spectrometer using DMSO- d_6 as solvent. Electrospray ionization mass (ESI-MS) measurements were carried out using impact HD instrument. IR spectra were recorded on NICOLET IS5 instrument using KBr plates. UV-vis spectra were recorded on a Shimadzu UV-2600 Spectrophotometer with a quartz cuvette (path length = 1 cm) at room temperature (r.t). Fluorescence spectra were recorded on Shimadzu RF-5301 PC spectrophotometer. For all the spectroscopic titrations, DMSO solution of **R1** (5×10^{-5} M) and aqueous solution of metal acetate and anions (1.5×10^{-3} M) were prepared.

Cell culture for RAW264.7 Macrophages for the bio imaging process

Bio imaging of living cells was performed with a Leica TCS SP5 X AOBS Confocal Fluorescence Microscope (Germany), and a 63x oil-immersion objective lens was used. The cell line RAW264.7 was provided by the Food Industry Research and Development Institute (Taiwan). RAW264.7 cells were cultured in Dulbecco's modified Eagle's medium (DMEM) supplemented with 10% fetal bovine serum (FBS) at 37 °C under an atmosphere of 5% CO_2 . Cells were plated on 18 mm glass coverslips and allowed to adhere for 24 h. Experiments to assess Zn^{2+} uptake were performed in TBS buffer with 10 μM of $\text{Zn}(\text{OAc})_2$ and incubated for 30 min at 37°C. The treated cells were washed by TBS buffer (3×2 mL) to remove remaining metal ions. Culture media (2 mL) was added to the cell culture, which was treated with a 10 μM solution of **R1** dissolved in DMSO. The samples were incubated at 37°C for 30 min. The culture media was removed, and the treated cells were washed with TBS buffer (3×2 mL) before observation. Experiments to assess H_2PO_4^- uptake were performed in TBS buffer with $(\text{CH}_3(\text{CH}_2)_3)_4\text{N}(\text{H}_2\text{PO}_4)$. Treat the above cells with 20 μM of $(\text{CH}_3(\text{CH}_2)_3)_4\text{N}(\text{H}_2\text{PO}_4)$ dissolved in sterilized TBS buffer (pH 7.4) and incubate for 60 min at 37°C. Wash the treated cells three times with 2 mL TBS buffer to remove the remaining $(\text{CH}_3(\text{CH}_2)_3)_4\text{N}(\text{H}_2\text{PO}_4)$. Confocal fluorescence imaging of cells was performed with a Leica TCS SP5 X AOBS Confocal Fluorescence Microscope (Germany), and a 63x oil-immersion objective lens was used. The cells were excited with a white light laser at 447 nm, and emission was collected at 502 ± 34 nm.

Syntheses of R1

1 mmol of 2, 5 thiophene-dicarboxaldehyde in anhydrous ethanol was added to the anhydrous ethanol solution of 2 mmol of isonicotinohydrazide. The above reaction mixture was allowed to reflux at 70 °C for 2 hrs. Completion of reaction was monitored through TLC. The precipitate formed was filtered in hot condition, washed with ethanol for three times and the product was dried. Yield: 80%. IR (KBr, cm^{-1}): 3431, 3213, 1646, 1544, 1295. ^1H NMR (DMSO- d_6 , 400 MHz δ ppm): 12.14 (s, 1H, NH), 8.79 (d, J = 4.80 Hz, 2H), 7.81 (d, J = 5.20 Hz, 2H), 8.67 (s, 1H, CH=N), 7.81-7.80 (d, 2H, Ar H), 7.53 (s, 1H, Ar H). ^{13}C NMR (DMSO- d_6 , 75 MHz δ ppm): 161.53, 150.32, 143.57, 140.97, 140.30, 131.79, 121.45. Mass (M+1): 379.0972 (calcd.) 379.0980 (observed).

Conclusion

In summary, we have developed a new dipodal N-acyl hydrazone receptor (**R1**) for the selective fluorescent sensing of Zn^{2+} ion, particularly zinc acetate. In presence of 2 eq. of Zn^{2+} ion, the colorless solution of free **R1** was turned into yellow color. Meanwhile, **R1**- Zn^{2+} complex showed strong absorption signal at 450 nm and fluorescence enhancement with two maxima at 502 nm and 534 nm. Further, the reversible and selective sensing of H_2PO_4^- ion was also successfully demonstrated using the insitu formed **R1**- Zn^{2+} complex. The fluorescence intensity at 502 nm and 534 nm was almost quenched in presence of H_2PO_4^- ion and the yellow color was turned into colorless. Other anions such as F^- , Cl^- , Br^- , AcO^- , CN^- , HSO_4^- and NO_3^- did not make significant influence in the fluorescence signal. Reversible sensing of phosphates with different basicity also studied using KH_2PO_4 , K_2HPO_4 and K_3PO_4 salts. In addition to that, acetate salts of Co^{2+} , Ni^{2+} and Cu^{2+} ions were showed obvious changes in the colorimetric and UV-vis titrations, thus forming only a ground state complex. The intracellular uptake of Zn^{2+} ion by **R1** and H_2PO_4^- ion by **R1**- Zn^{2+} complex also successfully tested in the living RAW 264.7 cells with the support of confocal microscope. TDDFT calculation was used to correlate the experimental observation.

Acknowledgements

One of the authors S.V thanks INSA for bilateral Exchange fellowship to visit National Chiao Tung University, Taiwan

Notes and references

- ^a Organic and Polymer Synthesis Laboratory, Department of Chemistry, National Institute of Technology, Tiruchirappalli 620 015, INDIA. *E-mail: velmathis@nitt.edu, svelmathi@hotmail.com.
- ^bDepartment of Applied Chemistry, National Chiao Tung University, Hsinchu, Taiwan, Republic of China.
- ^cDepartment of Chemistry, St. Joseph's College (Autonomous), Tiruchirappalli 620002.
1. P. A. Gale, S. E. Garcia-Garrido, J. Garric, *Chem. Soc. Rev.* **2008**, 37, 151.
2. J. Yoon, S. K. Kim, N. J. Singh and K. S. Kim, *Chem. Soc. Rev.* **2006**, 35, 355.
3. M. Formica, V. Fusi, L. Giorgi, M. Micheloni, *Coord. Chem. Rev.* **2012**, 256, 170.
4. S. J. Zhen, F. L. Guo, L. Q. Chen, Y. F. Li, Q. Zhang, C. Z. Huang, *Chem. Commun.* **2011**, 47, 2562.
5. D. Maity, T. Govindaraju, *Inorg. chem.* **2011**, 50, 11282.
6. N. Aksuner, E. Henden, I. Yilmaz, A. Cukurovali, *Sens. Actuators, A.* **2012**, 166-167, 269.
7. L. Wang, D. Ye, D. Cao, *Spectrochim. Acta, Part A.* **2012**, 90, 40.
8. S. Hu, S. Zhang, Y. Hua, Q. Tao, A. Wu, *Dyes. Pigments.* **2013**, 96, 509.
9. Q. Lin, P. Chen, J. Liu, Y. P. Fu, Y. M. Zhang, T. B. Wei, *Dyes. Pigments.* **2013**, 98, 100.

10. H. Zhou, J. Wang, Y. Chen, W. Xi, Z. Zheng, D. Xu, Y. Cao, G. Liu, W. Zhu, J. Wu, Y. Tian, *Dyes. Pigments*. **2013**, 98, 1.
11. T. Li, Z. Yang, Y. Li, Z. Liu, G. Qi, B. Wang, *Dyes. Pigments*. **2011**, 88, 103.
12. J. Huang, M. Tang, M. Liu, M. Zhou, Z. Liu, Y. Cao, M. Zhu, S. Liu, W. Zeng. *Dyes. Pigments*. **2014**, 107, 1.
13. D. Udhayakumari, S. Velmathi, Y. M. Sung, S. P. Wu, *Sens. Actuators, B*. **2014**, 198, 285.
14. Z. C. Xu, J. Yoon, D.R. Spring, *Chem. Soc. Rev.* **2010**, 39, 1996.
15. E. Kimura, T. Koike, *Chem. Soc. Rev.* **1998**, 27, 179.
16. G.Q. Xie, Y. J. Shi, F. P. Hou, H.Y. Liu, L. Huang, P. X. Xi, F. J. Chen, Z. Z. Zeng, *Eur. J. Inorg. Chem.* **2012**, 162, 327.
17. J. F. Zhu, W. H. Chan, A.W. M. Lee, *Tetrahedron Lett.* **2012**, 53, 2001.
18. Z. Xu, X. Liu, J. Pan, D. R. Spring, *Chem. Commun.* **2012**, 48, 4764.
19. X. Zhou, B. Yu, Y. Guo, X. Tang, H. Zhang, W. Liu, *Inorg. Chem.* **2010**, 49, 4002.
20. L. Li, Y.Q. Dang, H.W. Li, B. Wang, Y. Wu, *Tetrahedron Lett.* **2010**, 51, 618.
21. X.Y. Chen, J. Shi, Y.M. Li, F. L. Wang, X. Wu, Q.X. Guo, L. Liu, *Org. Lett.* **2009**, 11, 4426.
22. E. J. O'Neil, B. D. Smith, *Coord. Chem. Rev.* **2006**, 250, 3068.
23. D. Aldakov, P. Anzenbacher, *J. Am. Chem. Soc.* **2004**, 126, 4752.
24. T. D. Thangadurai, C. J. Lee, S. H. Jeong, S. Yoon, Y. G. Seo, Y-III Lee. *Microchemical J.* **2013**, 106, 27.
25. X. Zhao, K. S. Schanze, *Chem. Commun.* **2010**, 46, 6075.
26. X. Lou, D. Ou, Q. Li and Z. Li, *Chem. Commun.* **2012**, 48, 8462.
27. L. Zhong, F. Xing, Y. Bai, Y. Zhao, S. Zhu, *Spectrochim. Acta, Part A*. **2013**, 115, 370.
29. Z. Chen, L. Wang, G. Zou, X. Cao, Y. Wu, P. Hu, *Spectrochim. Acta, Part A*. **2013**, 114, 323.
30. P. Saluja, N. Kaur, N. Singh, D. O. Jang, *Tetrahedron Lett.* **2012**, 53, 3292.
31. X. Feng, Y. An, Z. Yao, C. Li, G. Shi, *ACS Appl. Mater. Interfaces*. **2012**, 4, 614.
32. S. Goswami, S. Paul and A. Manna, *RSC Adv.* **2013**, 3, 10639.
33. S. Goswami, A. Manna, S. Paul, K. Aich, A. K. Das and S. Chakraborty, *Dalton Trans.* **2013**, 42, 8078.
34. L. Fabbrizzi, N. Marcotte, F. Stomeo and A. Taglietti, *Angew. Chemie Int. Edn.* **2002**, 41, 3811.
35. L. Tang, M. Cai, P. Zhou, J. Zhao, K. Zhong, S. Hou and Y. Bian, *RSC Adv.* **2013**, 3, 16802.
36. R. K. Pathak, K. Tabbasum, A. Rai, D. Panda, C. P. Rao, *Anal. Chem.* **2012**, 84, 5117.
37. J. H. Lee, J. Park, M. S. Lah, J. Chin, J. I. Hong, *Org. Lett.* **2007**, 9, 3729.
38. W. H. Chen, Y. Xing, Y. Pang, *Org. Lett.* **2011**, 13, 1362.
39. B. B. Shi, Y. M. Zhang, T. B. Wei, Q. Lin, H. Yao, P. Zhang, X. M. You. *Sens. Actuators, B*. **2014**, 190, 555.
40. B. K. Datta, S. Mukherjee, C. Kar, A. Ramesh, G. Das. *Anal. Chem.* **2013**, 85, 8369.
41. L. J. Liang, X. J. Zhao and C. Z. Huang, *Analyst.* **2012**, 137, 953.
42. S. Suganya, H. J. Zo, J. S. Park, S. Velmathi, *Ind. Eng. Chem. Res.* **2014**, 53, 9561.
43. S. Suganya, S. Velmathi, D. MubarakAli, *Dyes. Pigments*. **2014**, 104, 116.
44. S. Suganya, J. S. Park, S. Velmathi, *Sens. Actuators, B*. **2014**, 190, 679.
45. D. Udhayakumari, S. Suganya, S. Velmathi, D. MubarakAli, *J. Mol. Recogn.* **2014**, 27, 151.
46. S. Devaraj, D. Saravanakumar, M. Kandaswamy. *Sens and Actuat. B* **2009**, 136, 13–19.
47. M. Hosseini, Z. Vaezi, M. R. Ganjali, F. Faridbod, S. D. Abkenar, K. Alizadeh, M. Salavati-Niasari. *Spectrochimica Acta Part A*. **2010**, 75, 978–982.
48. H. H. Hammud, A. Ghannouma, M. S. Masoud. *Spectrochimica Acta Part A*. **2006**, 63, 255–265.
49. X. Su and I. Aprahamian. *Chem. Soc. Rev.* **2014**, 43, 1963–1981.
50. L. Wang, W. Qin, W. Liu. *Inorg. Chem. Commun.* **2010**, 13, 1122–1125.
51. E. Runge, and E. K. U. Gross. Density-Functional Theory for Time-Dependent Systems. *Physical Rev. Lett.* **1984**, 52, 997–1000.
52. Gaussian 09, M. J. Frisch, G. W. Trucks, H. B. Schlegel, G. E. Scuseria, M. A. Robb, J. R. Cheeseman, G. Scalmani, V. Barone, B. Mennucci, G. A. Petersson, H. Nakatsuji, M. Caricato, X. Li, H. P. Hratchian, A. F. Izmaylov, J. Bloino, G. Zheng, J. L. Sonnenberg, M. Hada, M. Ehara, K. Toyota, R. Fukuda, J. Hasegawa, M. Ishida, T. Nakajima, Y. Honda, O. Kitao, H. Nakai, T. Vreven, J. A. Montgomery, Jr., J. E. Peralta, F. Ogliaro, M. Bearpark, J. J. Heyd, E. Brothers, K. N. Kudin, V. N. Staroverov, R. Kobayashi, J. Normand, K. Raghavachari, A. Rendell, J. C. Burant, S. S. Iyengar, J. Tomasi, M. Cossi, N. Rega, J. M. Millam, M. Klene, J. E. Knox, J. B. Cross, V. Bakken, C. Adamo, J. Jaramillo, R. Gomperts, R. E. Stratmann, O. Yazyev, A. J. Austin, R. Cammi, C. Pomelli, J. W. Ochterski, R. L. Martin, K. Morokuma, V. G. Zakrzewski, G. A. Voth, P. Salvador, J. J. Dannenberg, S. Dapprich, A. D. Daniels, O. Farkas, J. B. Foresman, J. V. Ortiz, J. Cioslowski, and D. J. Fox, Gaussian, Inc., Wallingford CT, **2009**.